

Ab initio molecular treatment of charge transfer by Si^{4+} ions in helium

M. C. Bacchus-Montabonel and P. Ceyzeriat

Laboratoire de Spectrométrie Ionique et Moléculaire, UMR 5579, CNRS et Université de Lyon I, 43, Boulevard du 11 Novembre 1918, 69622 Villeurbanne Cedex, France

(Received 5 March 1998)

Ab initio potential-energy curves and coupling matrix elements of the $^1\text{3}\Sigma$ and $^1\text{3}\Pi$ molecular states involved in the collision of the Si^{4+} multicharged ion on helium have been determined by means of configuration-interaction methods. The total and partial electron capture cross sections have been determined using a semiclassical approach in the 2-eV–60-keV laboratory energy range. A sharp resonance has been exhibited for a 45.455-eV collision energy. [S1050-2947(98)00808-7]

PACS number(s): 34.70.+e

I. INTRODUCTION

Low-energy electron capture by multiply charged ions with atomic hydrogen and helium has been shown to be an important process in controlled thermonuclear fusion research; in particular, the study of reactions involving carbon, oxygen and, more recently, boron has been stimulated by the need for precise information about impurity ion behavior. The charge transfer recombination process is also quite significant in astrophysical plasmas for many low-charged ions whose emission lines are used to provide direct information on the ionization structure of astronomical objects, and such reactions have been recognized to be possible ionization sources [1]. This is the case, for example, for silicon ions that are used to deduce electron temperature and density in emissive regions [2]. However, relatively little detailed work has yet been done on second-period elements. For silicon ions, in particular, charge-transfer recombination processes with atomic hydrogen have been investigated by means of model potential molecular methods using a one- [$\text{Si}^{2+}\text{-H}$ [3,4]; $\text{Si}^{4+}\text{-H(D)}$ [5]] or a two-active electron approach ($\text{Si}^{3+}\text{-H}$ [6]), but only one work has considered charge-transfer reactions with helium ($\text{Si}^{3+}\text{-He}$) [7].

We report in this paper on a complete *ab initio* molecular treatment of the $\text{Si}^{4+}\text{-He}$ electron capture process. To the best of our knowledge, neither an experimental nor a theoretical study has yet been done on this collisional system. All the molecular states involved in the collisional process have been considered in the molecular calculation: the entry channel $^1\Sigma^+ \{ \text{Si}^{4+} + \text{He}(1s^2)^1S \}$, the $^1\text{3}\Sigma$ and $^1\text{3}\Pi$ states correlated to $\{ \text{Si}^{3+}(3p)^2P + \text{He}^+(1s)^2S \}$, and the $^1\text{3}\Sigma$ states correlated to $\{ \text{Si}^{3+}(3s)^2S + \text{He}^+(1s)^2S \}$. The collision dynamics has been performed by means of semiclassical methods including electron-translation effects and taking into account the nonadiabatic radial couplings between molecular states as well as the rotational coupling matrix elements between Σ and Π levels.

II. MOLECULAR CALCULATIONS

The potential-energy curves have been determined for a large number of interatomic distances in the 2–30-a.u. range by means of MCSCF+CI (multiconfiguration self-consistent-field) calculations with configuration interaction

(CI) based on the CIPSI algorithm [8] (configuration interaction by perturbation of a multiconfiguration wave function selected iteratively). A nonlocal pseudopotential [9] has been used to represent the core electrons of the silicon atom. The calculations have been performed with configuration interaction spaces of about 200 determinants for the zeroth-order diagonalization Hamiltonian. Special care has been taken to construct sets of determinants providing the same level of accuracy over the whole distance range with a threshold $\eta = 0.001$ for the perturbation contribution providing a good description of the wave functions.

The basis of atomic functions used to represent silicon ions is a $9s7p2d$ basis of Gaussian functions contracted to $5s4p2d$, optimized from the basis sets of McLean and Chandler [10] on $\text{Si}^{3+}(3s)^2S$, $\text{Si}^{2+}(3s3p)^3P$, and $\text{Si}^{2+}(3s3d)^3D$ [7]. For helium, we took the $4s1p$ basis [11] optimized from the 6.311G** basis of Krishnan *et al.* [12].

The potential-energy curves of the $^1\text{3}\Sigma$ and $^1\text{3}\Pi$ states correlated to the entry channel $\{ \text{Si}^{4+} + \text{He}(1s^2)^1S \}$ are displayed, respectively, in Figs. 1 and 2. The asymptotic energy values are seen to be in a quite reasonable agreement with experiment [13]; the discrepancy is 0.11 eV for the $\text{Si}^{3+}(3p)$ level, and 0.26 eV for $\text{Si}^{3+}(3s)$ (Table I). The $^1\Sigma^+$ potentials show evidence of two main avoided crossings, a very sharp one at $R = 6.95$ a.u. between the entry channel and the $^1\Sigma^+ \{ \text{Si}^{3+}(3p)^2P + \text{He}^+(1s)^2S \}$ level and an inner one at $R = 4.45$ a.u. with the $^1\Sigma^+ \{ \text{Si}^{3+}(3s)^2S + \text{He}^+(1s)^2S \}$ exit channel. The $^1\Pi$ potential-energy curve appears very close to the $^1\Sigma$ entry and exit channels in the neighborhood of the external avoided crossing and could then lead to efficient transitions via rotational coupling. No evidence of any avoided crossing is displayed for $^3\Sigma$ and $^3\Pi$ states in Fig. 2, besides, as far as spin orbit effects may be neglected in the collision energy range of interest, the charge-transfer process may be driven by the singlet manifold only.

The radial coupling matrix elements between all pairs of states of the same symmetry have been calculated by means of the finite difference technique:

$$g_{KL}(R) = \langle \Psi_K | \partial / \partial R | \Psi_L \rangle = \lim_{\Delta \rightarrow 0} 1/\Delta \langle \Psi_K(R) | \Psi_L(R + \Delta) \rangle$$

with the parameter $\Delta = 0.0012$ a.u. as previously tested and using the silicon nucleus as origin of electronic coordinates.

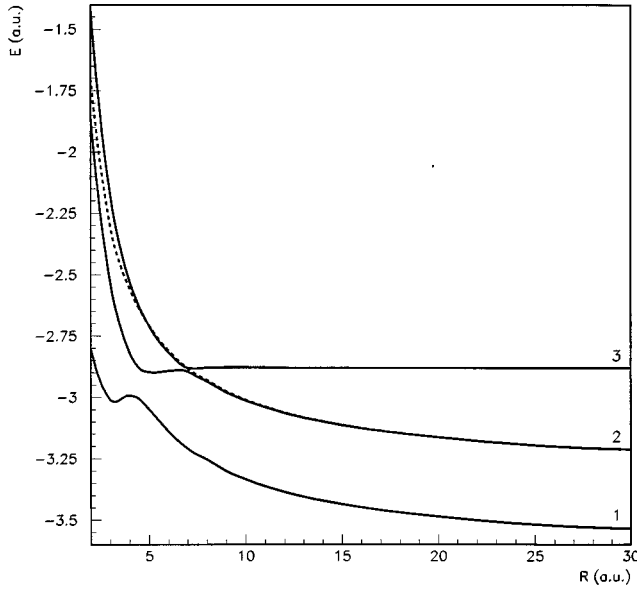


FIG. 1. Adiabatic potential-energy curves for the $^1\Sigma$ and $^1\Pi$ states of SiHe^{4+} . Solid lines, $^1\Sigma$; dashed lines, $^1\Pi$. (1) Σ state dissociating to $\{\text{Si}^{3+}(3s)^2S + \text{He}^+(1s)^2S\}$, (2) Σ, Π states dissociating to $\{\text{Si}^{3+}(3p)^2P + \text{He}^+(1s)^2S\}$, (3) Σ state dissociating to $\{\text{Si}^{4+} + \text{He}(1s^2)\}$.

The radial coupling matrix elements displayed in Fig. 3 present the same features as exhibited by the potential-energy curves with a sharp peak, 2.38 a.u. high, corresponding to the crossing at $R = 6.95$ a.u. and a smoother one, 0.74 a.u. high, corresponding to the inner crossing at $R = 4.45$ a.u. For reasons of numerical accuracy, we have performed a three-point numerical differentiation using calculations at $R + \Delta$ and $R - \Delta$ for a very large number of interatomic distances in the avoided crossing region, in particular for the sharp peaked coupling at about 7 a.u.

The rotational coupling matrix elements $\langle \Psi_K | iL_y | \Psi_L \rangle$ between $^1\Sigma - ^1\Pi$ and $^3\Sigma - ^3\Pi$ molecular states have been determined directly from the quadrupole moment tensor. The coupling matrix elements are presented in Fig. 4 and show clearly the interactions between the entry channel and the exit $^1\Sigma^+ \{\text{Si}^{3+}(3p)^2P + \text{He}^+(1s)^2S\}$ level in the neighborhood of the outer avoided crossing. The inner crossing, markedly smoother, appears as a small hump on the curve corresponding asymptotically to $\langle \Psi(3p)^2 | iL_y | \Psi(3p)^\Pi \rangle$ (see Fig. 4).

The determination of the quadrupole moment tensor between electronic wave functions allows the consideration of translation effects in the collision dynamics. In the approximation of the common translation factor [14], the radial and rotational coupling matrix elements between states Ψ_K and Ψ_L may indeed be transformed respectively into

TABLE I. Comparison of asymptotic energy values with experimental data.

	Calculation (eV)	Experiment [13] (eV)
$\text{Si}^{4+} + \text{He}$	0.0	0.0
$\text{Si}^{3+}(3p) + \text{He}^+$	-11.786	-11.677
$\text{Si}^{3+}(3s) + \text{He}^+$	-20.294	-20.553

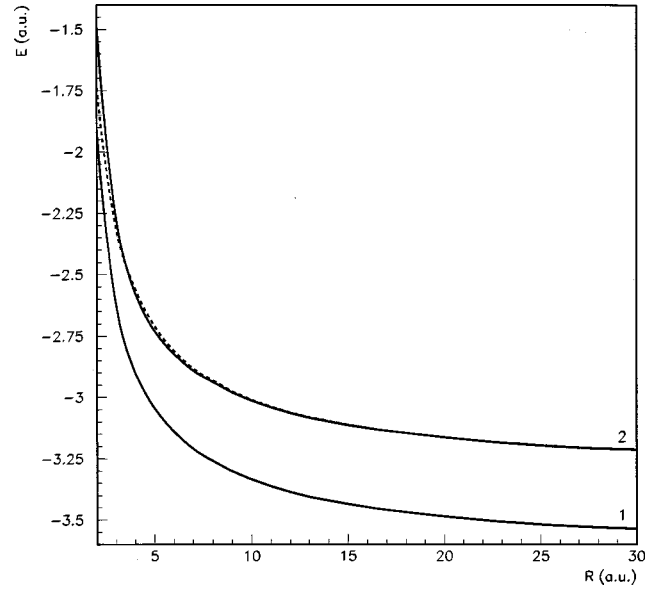


FIG. 2. Adiabatic potential-energy curves for the $^3\Sigma$ and $^3\Pi$ states of SiHe^{4+} . Solid lines, $^3\Sigma$; dashed lines, $^3\Pi$. (1) Σ state dissociating to $\{\text{Si}^{3+}(3s)^2S + \text{He}^+(1s)^2S\}$, (2) Σ, Π states dissociating to $\{\text{Si}^{3+}(3p)^2P + \text{He}^+(1s)^2S\}$.

$$\left\langle \Psi_K \left| \frac{\partial}{\partial R} - (\epsilon_K - \epsilon_L) z^2 / 2R \right| \Psi_L \right\rangle,$$

$$\langle \Psi_K | iL_y + (\epsilon_K - \epsilon_L) zx | \Psi_L \rangle,$$

where ϵ_K and ϵ_L are the electronic energies of states Ψ_K and Ψ_L , and z^2 and zx are the components of the quadrupole moment tensor. This expression, valid for any choice of electronic coordinates, has been used with the silicon nucleus as the origin of electronic coordinates.

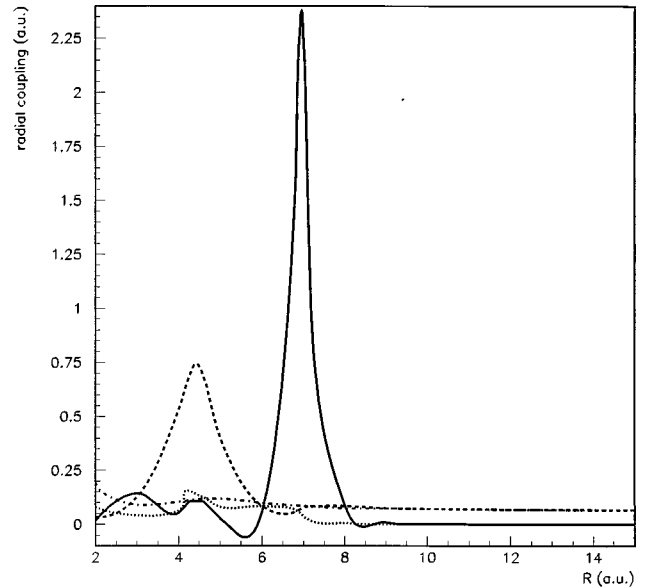


FIG. 3. Nonadiabatic radial coupling matrix element between $^{1,3}\Sigma$ states of SiHe^{4+} . Dashed line, g_{12} ; dotted line, g_{13} ; long-dashed line, g_{23} ; dash-dotted line g_{12} (triplet).

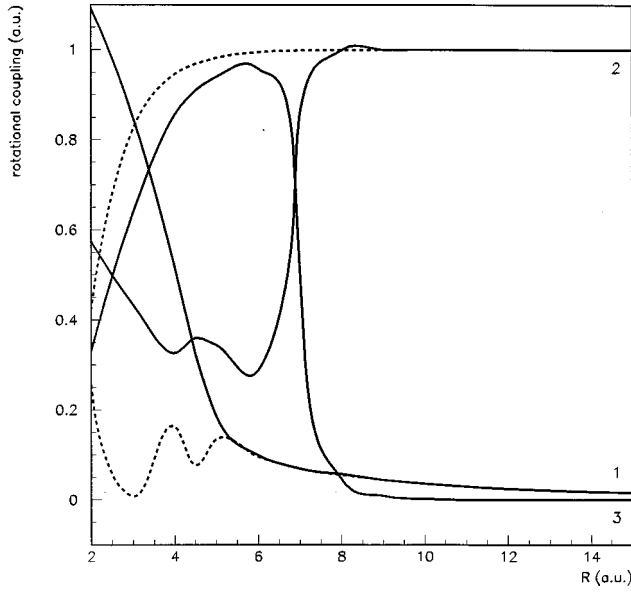


FIG. 4. Rotational coupling matrix elements between $1,3\Sigma$ and $1,3\Pi$ states of SiHe^{4+} . Solid lines, singlet; dashed lines, triplet. (1) $\langle \psi^\Sigma(3s) | iL_y | \psi^\Pi(3p) \rangle$, (2) $\langle \psi^\Sigma(3p) | iL_y | \psi^\Pi(3p) \rangle$, (3) $\langle \psi^\Sigma(ve) | iL_y | \psi^\Pi(3p) \rangle$.

III. COLLISION DYNAMICS

The collision dynamics has been treated by a semiclassical method using the EIKONXS program [15] based on an efficient propagation method in the 2 eV–60-keV laboratory energy range. In order to evaluate the influence of translation effects on the capture cross sections, we have performed two calculations, with and without the translation correction factor as explicated in the previous paragraph. The results are displayed in Fig. 5 and show clearly a quite weak influence of translation effects for this system; the relative variation is always lower than 4%, even for the higher collision energies.

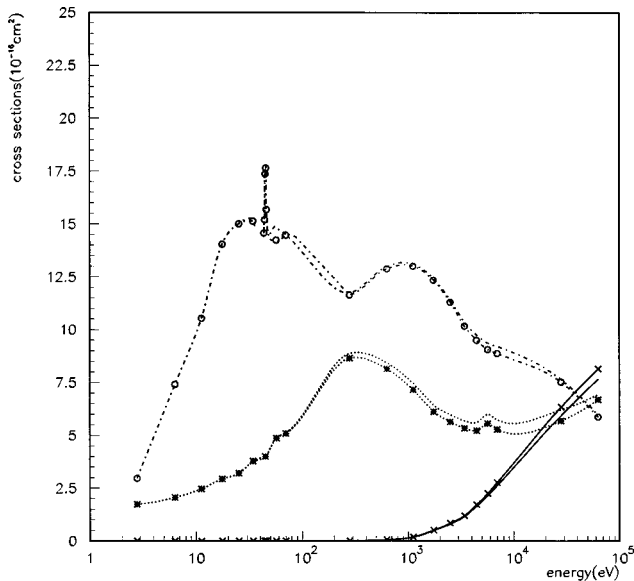


FIG. 5. Translation effect on the partial cross sections on the $\{\text{Si}^{3+} + \text{He}^+\}$ levels with respect to laboratory energies. Markers, with translation effect; no markers, without translation effect. Solid lines, σ_{3s}^Σ ; dotted lines, σ_{3p}^Π ; dash-dotted lines, σ_{3p}^Σ .

TABLE II. Partial and total cross sections for the $\text{Si}^{4+} + \text{He} \rightarrow \text{Si}^{3+} + \text{He}^+$ charge-transfer process (in 10^{-16} cm^2).

E_{lab} (eV)	σ_{3p}^Σ	σ_{3p}^Π	σ_{3s}^Σ	σ_{3p}^{tot}	σ^{tot}
2.806	2.974	1.733	0.0	4.707	4.707
6.333	7.411	2.054	0.0	9.466	9.466
11.223	10.538	2.469	0.0	13.01	13.01
17.557	14.044	2.946	0.0	16.99	16.99
25.253	14.997	3.206	0.0	18.20	18.20
34.392	15.122	3.782	0.0	18.90	18.90
43.772	14.572	4.013	0.0	18.58	18.58
44.333	15.179	3.738	0.0	19.33	19.33
44.894	17.367	3.993	0.0	21.36	21.36
45.455	17.638	4.322	0.0	22.46	22.46
46.016	15.680	4.126	0.0	19.81	19.81
56.839	14.227	4.871	0.0	19.10	19.10
70.147	14.471	5.087	0.0	19.56	19.56
280.67	11.649	8.647	0.006	20.30	20.30
631.40	12.886	8.137	0.055	21.02	21.08
1.12×10^3	13.010	7.156	0.187	20.17	20.35
1.75×10^3	12.345	6.115	0.505	18.46	18.96
2.52×10^3	11.304	5.661	0.843	16.96	17.81
3.44×10^3	10.171	5.341	1.198	15.51	16.71
4.49×10^3	9.498	5.230	1.724	14.73	16.45
5.68×10^3	9.062	5.567	2.246	14.63	16.87
7.01×10^3	8.875	5.288	2.768	14.16	16.93
28.1×10^3	7.520	5.702	6.346	13.22	19.57
63.2×10^3	5.882	6.700	8.143	12.58	20.72

To some extent, such a calculation may also provide an evaluation of the precision of our calculation as it exhibits the influence of the origin of electronic coordinates in the collision dynamics. A precision of about 10% or even less may be accepted for this calculation; this is quite accurate

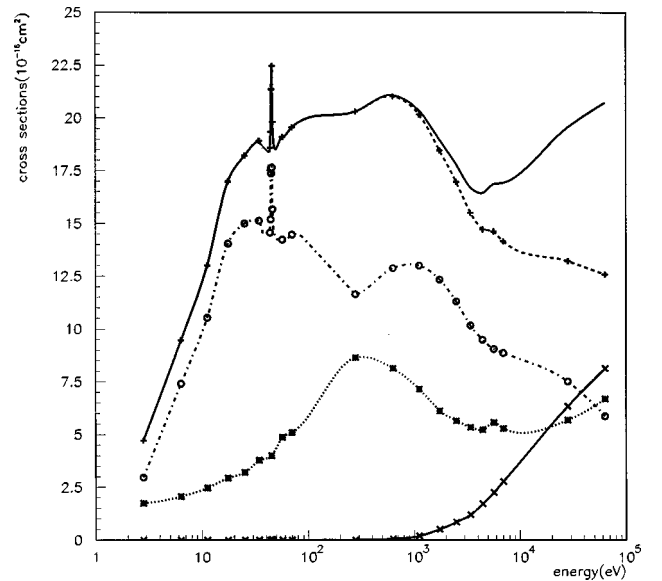


FIG. 6. Total and partial cross sections on the $\{\text{Si}^{3+} + \text{He}^+\}$ levels with respect to laboratory energies. Solid line at bottom, σ_{3s}^Σ ; dotted line, σ_{3p}^Π ; dash-dotted line, σ_{3p}^Σ ; dashed line, σ_{3p}^Π ; solid line at top, σ_{tot} (no markers).

compared to experimental or other theoretical works [16,11] owing to the low convergence threshold ($\eta=0.001$) and the large number of points involved in the molecular calculation, in particular, for the determination of the radial coupling matrix elements.

Taking account of translation effects, the total and partial capture cross sections are presented in Table II and sketched in Fig. 6. Up to collision energies of about 1 keV, the value of the partial cross section on the $\{\text{Si}^{3+}(3s)+\text{He}^+\}$ level remains almost zero because of the relatively smooth interaction and the energetic gap between this state and the entry channel. For higher energies, the inner crossing may be efficient and the $\text{Si}^{3+}(3s)$ state may be populated leading to cross sections increasing with energy. The charge-transfer recombination process is, however, driven mainly by the outer crossing and important cross sections for capture on the $^1\Sigma^+ \{\text{Si}^{3+}(3p)+\text{He}^+\}$ level are exhibited. As expected from the potential-energy curves, the rotational coupling is nevertheless not negligible at all, as observed on the partial cross section σ_{3p}^{Π} on the $^1\Pi \{\text{Si}^{3+}(3p)+\text{He}^+\}$ level, which reaches values up to $8.43 \cdot 10^{-16} \text{ cm}^2$ at its maximum. We may note the existence of a very narrow resonance for the σ_{3p}^{Σ} capture cross section for an energy of 45.455 eV. Such a

curious feature may be attributed to a very important contribution of one particular partial wave, as exhibited on the $\text{O}^{2+}+\text{He}$ collisional system [17] and has been already noticed for $\text{N}^{3+}-\text{H}$ [18] and $\text{N}^{5+}-\text{H}$ [19]. Taking apart the resonance, the total cross section shows a maximum at about 600 eV, then decreases as the σ_{3p}^{tot} cross section until the contribution of the σ_{3s}^{Σ} partial cross section lets it increase again.

IV. CONCLUDING REMARKS

This work provides accurate *ab initio* potential energy curves, radial and rotational coupling matrix elements for the $\text{Si}^{4+}+\text{He}$ collisional system. Both radial and rotational couplings have been shown to be necessary in a fair description of the charge-transfer recombination process, although translation effects remain weak all over the whole collision energy range. The collision dynamics is yet essentially driven by means of the radial coupling interaction between the entry channel and the $^1\Sigma^+ \{\text{Si}^{3+}(3p)+\text{He}^+\}$ level leading to relatively high values for the partial σ_{3p}^{Σ} cross section, which presents a remarkable resonance at a 45.455 eV collisional energy.

-
- [1] S. L. Baliunas and S. E. Butler, *Astrophys. J. Lett.* **235**, L45 (1980).
 - [2] H. Nussbaumer, *Astron. Astrophys.* **155**, 205 (1986).
 - [3] M. Gargaud, R. McCarroll, and P. Valiron, *Astron. Astrophys.* **106**, 197 (1982).
 - [4] R. McCarroll and P. Valiron, *Astron. Astrophys.* **53**, 83 (1976).
 - [5] M. Gargaud and R. McCarroll, *J. Phys. B* **21**, 513 (1988); M. Pieksma, M. Gargaud, R. McCarroll, and C. C. Havener, *Phys. Rev. A* **54**, R13 (1996).
 - [6] B. Herrero, I. L. Cooper, and A. S. Dickinson, *J. Phys. B* **29**, 5583 (1996).
 - [7] P. Honvault, Doctorate thesis, University of Lyon, France, 1995.
 - [8] B. Huron, J. P. Malrieu, and P. Rancurel, *J. Chem. Phys.* **58**, 5745 (1973).
 - [9] M. Pélissier, N. Komih, and J. P. Daudey, *J. Comput. Chem.* **9**, 298 (1988).
 - [10] A. D. McLean and G. S. Chandler, *J. Chem. Phys.* **72**, 5639 (1980).
 - [11] M. C. Bacchus-Montabonel, *Phys. Rev. A* **46**, 217 (1992).
 - [12] R. Krishnan, J. S. Binkley, R. Seeger, and J. A. Pople, *J. Chem. Phys.* **72**, 650 (1980).
 - [13] S. Bashkin and J. O. Stoner, *Atomic Energy Levels and Grotian Diagrams* (North-Holland, Amsterdam, 1975).
 - [14] L. F. Errea, L. Mendez, and A. Riera, *J. Phys. B* **15**, 101 (1982).
 - [15] R. J. Allan, C. Courbin, P. Salas, and P. Wahnon, *J. Phys. B* **23**, L461 (1990).
 - [16] M. Druetta, T. Bouchama, and S. Martin, *Nucl. Instrum. Methods Phys. Res. B* **40/41**, 50 (1989).
 - [17] M. Gargaud, M. C. Bacchus-Montabonel, and R. McCarroll, *J. Chem. Phys.* **99**, 4495 (1993).
 - [18] M. Rittby, N. Elander, E. Brändas, and A. Bárány, *J. Phys. B* **17**, L677 (1984).
 - [19] N. Shimakura and M. Kimura, *Phys. Rev. A* **44**, 1659 (1991).